COMPUTATIONAL MECHANICS 2021
36th conference with international participation
Srní
November 8 - 10, 2021

Dynamic mode decomposition and its application to the flutter analysis

J. Valášek, P. Sváček

Faculty of Mechanical Engineering, Czech Technical University in Prague, Karlovo nám. 13, Praha 2, 121 35

In this paper the dynamic mode decomposition (DMD) method is introduced. It is a data-driven and model-free method which decomposes a given set of signals to DMD modes and associated DMD eigenvalues, [2, 4]. Thus it offers a very interesting alternative to the proper orthogonal decomposition (POD) and similar methods usually used for the low-rank representation of the high-dimensional data. The advantage of DMD is better physical interpretation of the decomposition as the DMD modes have monofrequency content and the complex DMD eigenvalues provide the frequency as well as the growth/decay rate of particular mode, [4]. Moreover the DMD has solid theoretical underpinnings given by the Koopman operator, [2]. The disadvantage of DMD is a relative ambiguity of DMD mode selection which are not sorted as in the case POD decomposition, [1]. Finally an application example of the DMD analysis to the numerical simulation of flutter vibrations is presented.

DMD theory In the beginning let us assume that we study dynamical system of the form

$$\frac{\partial \mathbf{x}}{\partial t} = \mathbf{f}(\mathbf{x}, t, \mu), \tag{1}$$

where $\mathbf{x}(t) \in \mathbb{R}^n$ is a state vector at time t, μ represents parameters of the system and function $\mathbf{f}(\cdot)$ is generally nonlinear. Further we denote $\mathbf{x}_k = \mathbf{x}(t_k)$ as solution of Eq. (1) at time instant t_k (for example assuming $t_k = k \cdot \Delta t$). The states $\mathbf{x}_k$ are typically very large and they can arise from the spatial discretization of a partial differential equation or they can be collected from measurements of the dynamical system. Next we have got a data set $\mathcal{D}$ consisting of $\mathcal{D} = \{\mathbf{x}_1, \ldots, \mathbf{x}_N\}$ for which we would like to find low-dimensional representation.

The DMD method is based on the matrix $\mathbb{A}$ describing time development of the system in the form

$$\mathbf{x}_{k+1} = \mathbb{A}\mathbf{x}_k, \qquad k \in \{1, \ldots, N-1\} \tag{2}$$

as best fit in least-square sense, i.e., minimizing

$$\sum_{k=1}^{N-1} ||\mathbf{x}_{k+1} - \mathbb{A}\mathbf{x}_k||_2. \tag{3}$$

It is now clear from Eq. (2) that the DMD actually locally linearizes the original system (1), [2]. Quite interestingly, the DMD method can be theoretically viewed as the finite-dimensional approximation of the Koopman operator. The Koopman operator is a linear, infinite-dimensional operator that precisely represents the nonlinear operator of the dynamical system with finite dimension, [2].

The dynamics of system (1) (or more accurately the dynamics hidden in the data set $\mathcal{D}$) is given by the DMD matrix $\mathbb{A}$. The key to it (and the key of the DMD) is to perform the

eigendecomposition of matrix $\mathbb{A}$ to eigenvalues λ_i and eigenvectors $\mathbf{\Phi}_i$. Then the analyzed state-space trajectory (given by $\mathcal{D}$) can be reproduced according to the formula

$$\mathbf{x}(t_{k+1}) = \mathbf{x}_{k+1} \approx \mathbb{A}^k \mathbf{x}_1 = \sum_{i=1}^{N-1} \mathbf{\Phi}_i \exp(\omega_i\, t_k)\, b_i, \tag{4}$$

where ω_i are approximate continuous-time eigenvalues given by $\omega_i = \ln(\lambda_i)/\Delta t$ and $\mathbf{b} = (b_i)$ are the initial coefficients of mode participation for each DMD mode, i.e., $\mathbf{b} = \mathbf{\Phi}^\dagger \mathbf{x}_1$ with † notation of pseudo-inverse. The real and the imaginary part of ω_i provides us information about the exponential growth/decay rate and the frequency content of the particular mode, respectively, see [4].

In practice the DMD matrix is replaced by the projection of the matrix $\mathbb{A}$ onto first r left-singular vectors obtained by singular value decomposition (SVD) and corresponding to the biggest r singular values of $\mathbb{A}$, i.e., by matrix $\tilde{\mathbb{A}}$. Then also the summation in formula (4) is typically restricted to $M \ll r$, i.e., it is enough to choose a few dominant DMD modes (here M modes) acceptably representing the system dynamics, [2].

In next paragraph we shortly present the numerical simulation on which results the DMD was applied.

FSI simulation Numerical simulation of flow-induced vibration of vocal folds (VFs) with the full channel configuration was conducted with in-house solver described in [5]. The VF geometry and simulation parameters are based on article [5]. Particularly, the constant time step Δt is chosen as $4 \cdot 10^{-5}$ s and the inlet velocity $v_{\text{in}} = 1.98$ m/s is prescribed with the aid of penalization parameter $\epsilon = \frac{1}{2000}$ s/m. Such choice of the inlet velocity together with the penalization parameter exceeds the critical flutter velocity estimated to be $v_{\text{crit}} \approx 1.9$ m/s, [6].

Fig. 1 shows the VF displacement recorded at the top point of bottom VF. The gradual increase of vibration amplitude can be observed when the increase in last 0.05 s has obviously the exponential character typical for flutter phenomenon. At time instant $t = 0.2956$ s the simulation failed due to too distorted computational fluid mesh. This is a big disadvantage of ALE method and an open issue for the simulation of healthy human phonation.

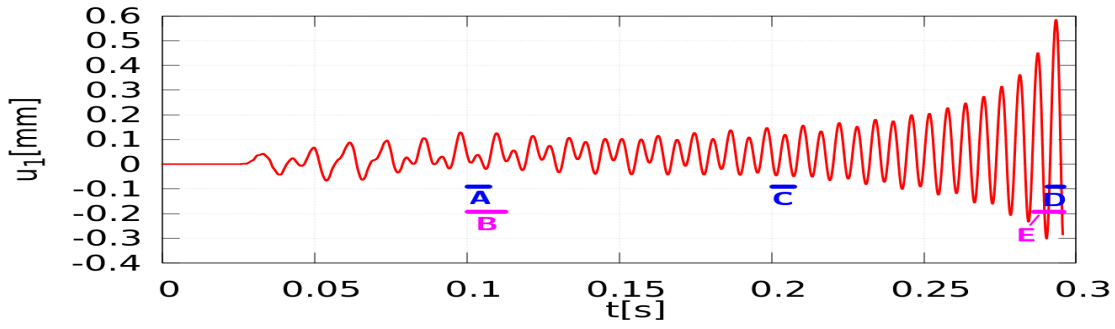

Fig. 1. VF displacement in x-direction monitored at point $S = [4.99; -0.505]$ mm. Five different time intervals are chosen for the application of DMD, marked by letters A-E

DMD application Here we apply the DMD on the numerical approximation of structural displacements $\mathbf{u}_h$ only. We choose 5 time intervals of 150 or 300 time steps covering the one or two periods of the most dominant frequency, see Fig. 1. The SVD is truncated such that all singular values greater than 10^{-3} are kept. The DMD mode with the highest mode participation measured as $z_i = |\sum_{k=1}^{N-1} \exp(\omega_i\, t_k)\, b_i|$ is chosen together with the DMD modes satisfying $z_i > 0.1 \cdot z_{\max}$, see [1].

The data sets from five different time intervals as shown in Fig. 1 are chosen. The DMD decomposition is performed for each of them and the chosen statistics are listed in Table 1. In all cases the DMD mode with frequency ≈ 168 Hz is present, in cases A, B, D is the dominant one. In cases B and E the highest contribution is associated with the mode representing asymmetry of the solution and having significant growth rate and rather unimportant frequency content. Formula (4) can be also used for the future state prediction for choice $k > N$. Employing this DMD feature the DMD prediction can be compared with the numerical solution in the cases A, B, C. The L^2 norm of the error e_{pred} of the DMD prediction for $k = N + 150$ (i.e., at the future 150^{th} time step) against the simulation is listed in the fifth column of Table 1. The reasonable agreement is achieved in case C, cases A and B fit well the given data sets but the correct prediction would need to better represent the interplay of two natural eigenmodes in the training data set. Similar problematic behaviour exhibits prediction in case E where the dominant DMD mode has too large growth rate which extrapolation gives wrong prediction clearly visible by eye. Omitting this dominant mode with excessive growth rate leads to an expectable DMD prediction.

Table 1. Five different data sets are analyzed by the DMD. The third column shows number of selected DMD modes. The error e_{pred} can not be computed in cases D and E as there is no simulation results to compare with

interval	time steps	# DMD modes	ω of the dominant mode	$e_{\text{pred}} \cdot 10^{-3}$
A	150	6	$5.81 + 168.5 \cdot 2\pi \cdot i$	1.3096
B	300	6	$53.2 + 5.8 \cdot 2\pi \cdot i$	1.2364
C	150	4	$9.8 + 168.5 \cdot 2\pi \cdot i$	0.47357
D	150	5	$65.69 + 167.3 \cdot 2\pi \cdot i$	'small'
E	300	5	$1000.5 + 101.5 \cdot 2\pi \cdot i$	'big'

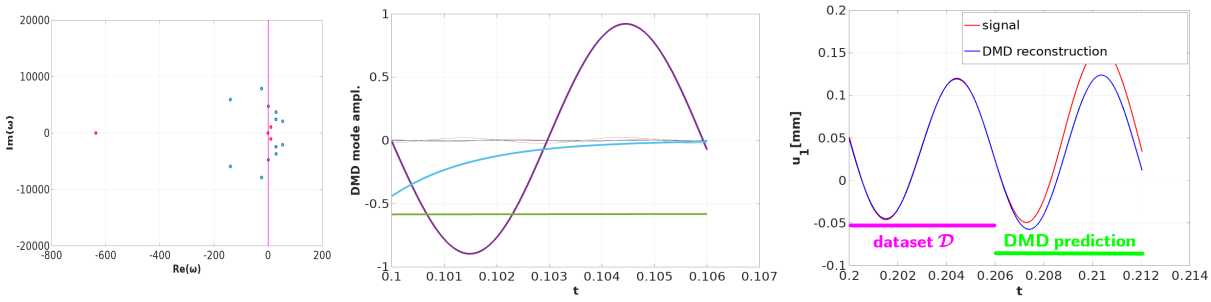

Fig. 2. (*Left*) DMD approximation of continuous-time eigenvalue spectrum. Vertical magenta line is the imaginary axis, i.e., stability boundary. The selected eigenvalues are highlighted by red circles. (*Middle*) Time behaviour of DMD mode participation coefficients (i.e., amplitudes). Three bold lines represents four selected DMD modes as the complex conjugated modes have the same real part of time behaviour. (*Right*) Comparison of the original displacement and the DMD prediction at point S. The state-space trajectory is reconstruction in time interval $0.2 - 0.206$ s (i.e., it is the data set) and the trajectory is predicted by the DMD based on Eq. (4) in time interval $0.206 - 0.212$ s. *All results concern case C*

Figs. 2 and 3 show more details about the DMD analysis for case C. The mentioned graphs for other cases are similar. Interestingly, the DMD mode with frequency ≈ 168 Hz is different from eigenmodes obtained by modal analysis. Its frequency lies between the second and the third natural eigenfrequency (155.8 Hz and 179.9 Hz) suggesting it is a vibration pattern arisen by merging of these two eigenmodes as it is typical for flutter phenomenon, see [7].

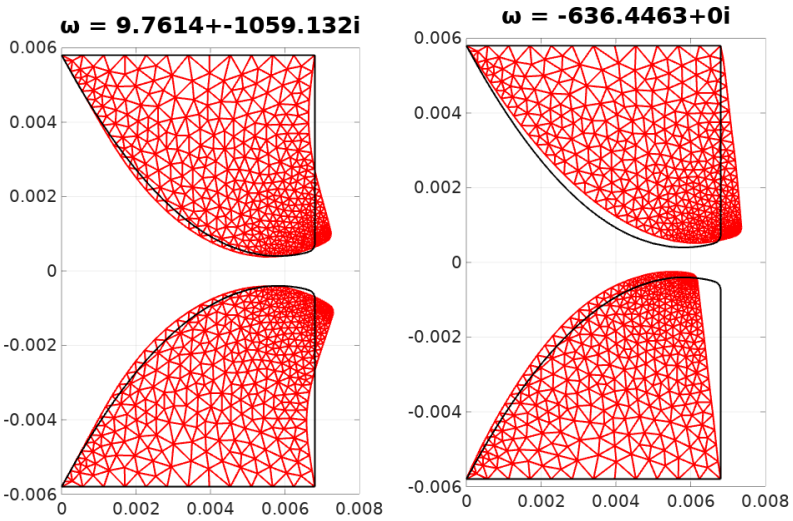

Fig. 3. Two selected DMD modes in case C. The *left* DMD mode has significant growth rate and frequency content 168.45 Hz. The relevance of the *right* DMD mode rapidly decaying with time as $Re(\omega) \ll 0$ and it has no frequency content, i.e., it helps to reconstruct the simulation asymmetry in the given data set only

Conclusion The DMD method is very interesting allowing us to uncover dynamics of given system without deep knowledge of it. The data set which it tries to reconstruct can be obtained by measurements or simulations. Therefore the DMD method has reached a lot of attention and many improvements of it have been developed, see e.g. [3]. Here it was applied on the flow-induced vocal fold vibrations. The presented analyses show that DMD can not be used as the all-able black-box but rather a little parameter tuning is needed.

Acknowledgements

Authors are grateful for support provided by *Grant No. GA19-04477S* of Czech Science Foundation and by *Grant No. SGS19/154/OHK2/3T/12* of the CTU in Prague.

References

[1] Kou, J., Zhang, W., An improved criterion to select dominant modes from dynamic mode decomposition, European Journal of Mechanics-B/Fluids 62 (2017) 109-129.

[2] Kutz, J. N., Brunton, S. L., Brunton, B. W., Proctor, J. L., Dynamic mode decomposition: Data-driven modeling of complex systems, Society for Industrial and Applied Mathematics, 2016.

[3] Noack, B. R., Stankiewicz, W., Morzyski, M., Schmid, P. J., Recursive dynamic mode decomposition of transient and post-transient wake flows, Journal of Fluid Mechanics 809 (2016) 843-872.

[4] Tu, J. H., Rowley, C. W., Luchtenburg, D. M., Brunton, S. L., Kutz, J. N., On dynamic mode decomposition: Theory and applications, Journal of Computational Dynamics 1 (2) (2014) 391-421.

[5] Valášek, J., Sváček, P., Horáček, J., On suitable inlet boundary conditions for fluid-structure interaction problems in a channel, Applications of Mathematics 64 (2) (2019) 225-251.

[6] Valášek, J., Sváček, P., Horáček, J., The influence of penalization inlet boundary condition on the stability boundary, Proceedings of the conference Computational Mechanics 2019, Srní, University of West Bohemia, 2019, pp. 212-215.

[7] Zhang, Z., Neubauer, J., Berry, D. A., Physical mechanisms of phonation onset: A linear stability analysis of an aeroelastic continuum model of phonation, The Journal of the Acoustical Society of America 122 (4) (2007) 2279-2295.